J. Ind. Geophys. Union (January 2017)
v.21, no.1, pp: 58-66

Simulation Results for Southern Indian Ocean (SIO) Using Ocean Model

A.P.Mishra[1, 2] and A.C.Pandey[1]

[1]Department of Atmospheric and Ocean Studies, Faculty of Science, Nehru Science Centre, University of Allahabad, Allahabad-211002

[2]Central Water Commission, Sewa Bhawan, R.K.Puram, New Delhi-110066

*Corresponding Author: anshu_ms@yahoo.com

ABSTRACT

A z-coordinate Modular Ocean Model (herein after referred as MOM3) has been implemented for global domain forced by NCEP/NCAR wind stress climatologies and executed for twenty five years. Several results of interest were analysed mainly for Southern Indian Ocean (SIO) (60°S-10°N, 30°E-120°E) including Antarctic Circumpolar Current (ACC) region of Southern Ocean (SO) from the output of the above model. The fidelity of the model is examined for varieties of phenomenon viz: surface elevation, horizontal circulations/vertical velocities at sub-surface, property transport including statistical estimation of Sea Surface Temperature (SST). The Results indicate that model produces strong variability of vertical velocity in the deeper ocean showing inability of z level model for bottom boundary layer correctly whereas the strength of the subsurface currents decays in comparison to the preceding depth circulation. It is noticed that in the upper ocean, the zonal transports are eastwards that may directly follow the surface currents. Statistical analyses include the estimation of model Error (ME), Correlation Coefficient (CC) denoted by R and Skill Score (SS) between model & observed SST data and result showing high correlation (R=0.94) with ME between 0 to 1^0C. CC and SS suggests the success of model up to some extent. As seen from the R values, which are close to 1 over most of the model domain, is thought to be SST is simulated well.

Key words: Wind Stress, ACC, Sub surface horizontal circulation, Sea Surface Temperature, Vertical Velocity and Statistical Analyses.

INTRODUCTION

The Southern Ocean (SO) plays a very important part in the general circulation of the world ocean and consequently the global climate system. Despite the recent advances in the understanding of SO, many questions remain unanswered. One reason is that the region is a particularly remote one with bad weather conditions and sea ice, which makes the collection of insitu data difficult (Best et al., 1999). Modelling SO is thus analytically somehwhat intractable and resources must be had to be based on/ taken from numerical methods (Killworth and Nanneh, 1994). There has been a controversial issue on the choice of a vertical coordinate system for use in a numerical model like Modular Ocean Model (MOM) in the ocean modelling community. The geopotential or z-level coordinate is the simplest and has been widely used in the past. However, z-level models must represent the real bathymetry by a series of steps, which may lead to large truncation errors over steep topography (Gerdes 1993; Adcroft, Hill and Marshall 1997; Gnanadesikan and Pacanowski 1997; Sheng et al., 1998).

In this study, our interest is to see the performance of the above model and to see the improvements over the existing studies/observation. In an attempt to reconcile some of the analyses/results from the present model for SIO/SO in response to wind forcing, we have examined horizontal circulation & vertical velocities (VV) at the sub-surface, property transport, SST using correlation and statistical measure from the output of the model and to possibly overcome the limitations of the observation based studies with the goal of obtaining a more complete physical understanding of the ocean dynamics and processes. Further, SST, being an important indicator of the state of the earth's climate system and its precise information, is very essential for climate monitoring, research and prediction (Reynolds et al., 2002) with focus on quantitative statistical measures between SST values of the model and observation. Moreover, VV diagnosed here is important as its measurements in the ocean are scarce (Thurnherr, 2011) and to study its variations, it is natural to quantify the VV variability and its distribution at the sub-surface and the processes responsible for such distribution. For instance, the equatorial upwelling that represents probably the largest mean VV is about 10^{-3} cm/s (Wyrtki, 1981) and in the deep oceans, the mean value of VV is much smaller (about 10^{-5}cm/s) (Munk, 1990). Spatial maps of different measures were shown/ generated to examine model performance.

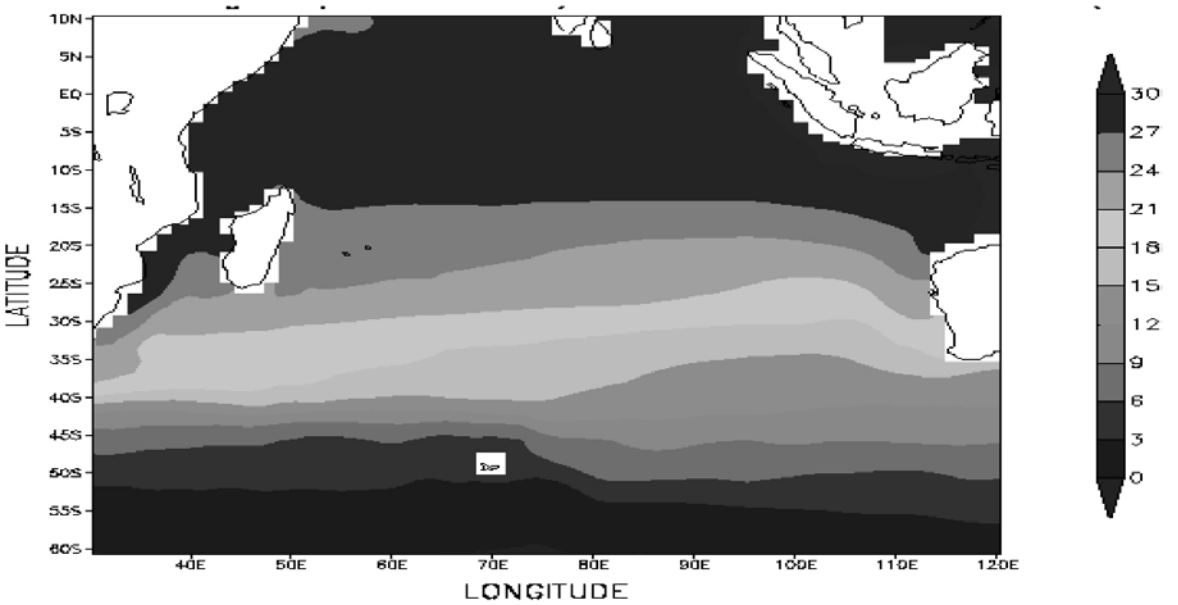

Figure 1. Six year average Model Surface Elevation Field (Units are in c.m.). The contour interval is 3 cm.

METHODOLOGY AND MODEL SETUP

Model and formulation

The version 3 of GFDL Modular Ocean Model [Pacanowski, Dixon and Rosati, 1993; Huang and Schneider 1995; Schneider et al., 1999] uses the Boussinesq and traditional approximations and allows the use of the rigid-lid and free-surface methods. It allows many types of mixing including horizontal mixing along surfaces of constant density and can be coupled to atmospheric models. The horizontal mixing of tracers and momentum is Laplacian. The momentum mixing uses the space-time dependent scheme of Smagorinsky (1963) and the tracer mixing uses Redi (1982) diffusion along with Gent and McWilliams (1990) quasi-adiabatic stirring. The zonal resolution is 1.5° while the meridional resolution is 0.5° between 10°N and 10°S, gradually increasing to 1.5° at 20°N and 20°S. There are 25 levels in the vertical with 17 levels in the upper 450 meters of the ocean. The model is forced by the long term mean surface wind stress from the National Center for Environmental Prediction (NCEP)-National Center for Atmospheric Research (NCAR reanalysis) (Kalnay et al., 1996). The original surface reanalysis is on an irregular grid with a zonal resolution of 1.875° and Gaussian latitudes of grid spacing less than 2°, and is linearly interpolated to the OGCM grids. The vertical mixing scheme is non-local K-Profile Parameterization (KPP) of Large, McWilliam and Doney 1994. The model surface salinity is relaxed to Levitus (1982) monthly climatology. Surface heat flux is also relaxed to Levitus (1982) climatology and relaxation time is 100 days. Model variables, set of equations, constants, coefficients and depth to the grid point used in the model are described in an earlier study (Mishra et al., 2010). The four 3-D prognostic variables of the model are zonal and meridional components of velocity (u, v), temperature (T) and salinity (S). The diagnostic variables are vertical velocity (ω) and density (ρ). In order to suppress the fast moving surface gravity waves, the rigid lid approximation is employed (i.e. $\omega=0$ at the surface $z=0$).

Experiment detail, Simulation domain and Study Region

The model is initialized from an ocean at rest with climatological temperature and salinity and then spun up for twenty five years under NCEP-NCAR climatological wind stress forcing. Initial condition is taken from annual mean temperature and salinity field without motion (Levitus, 1982). The monthly output of the model is saved and analyzed for SIO. Simulation domain of the model is that of the world oceans spanning from (74.25°S to 65°N, 180°W-180°E) and the analysis region includes SIO region including SO spanning from 30°E-120°E, 60°S-10°N.

RESULTS AND DISCUSSIONS

Surface Elevation, Horizontal Circulation and Vertical Velocities

Figure 1 shows the model climatology (last 6 year model run) of the surface elevation field in the Southern Indian Ocean region. We see that the surface elevation field shown in figure 1 is quite smooth and also the surface flow from the Indian Ocean into Madagascar near Somali

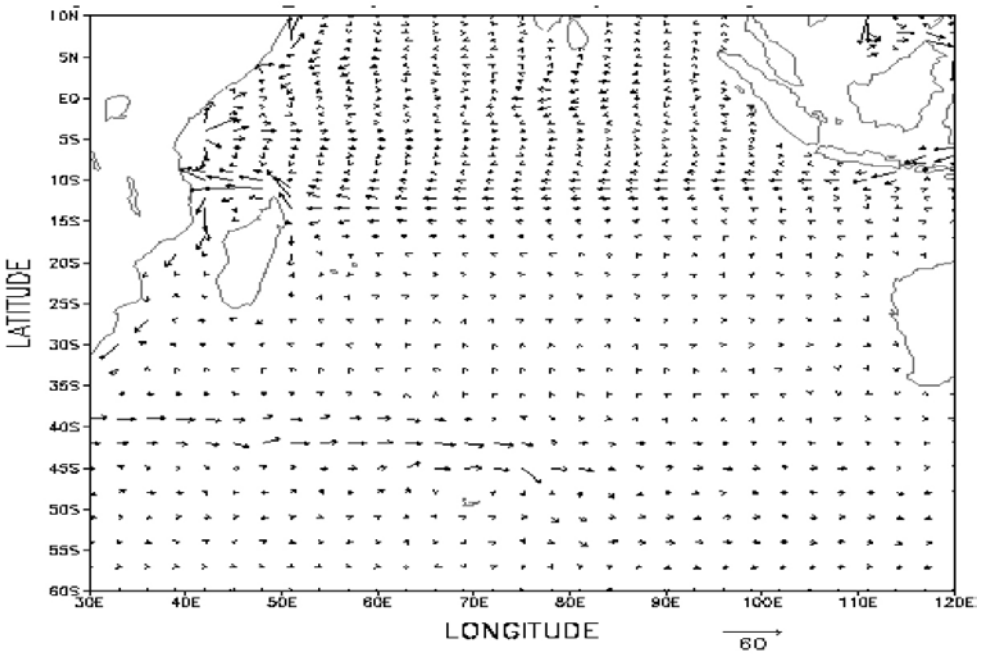

Figure 2. (a) Six year average horizontal circulation (cm/s) at 97.5 m. Arrow length of 0.5 cm represents current speed of 60 cm/s.

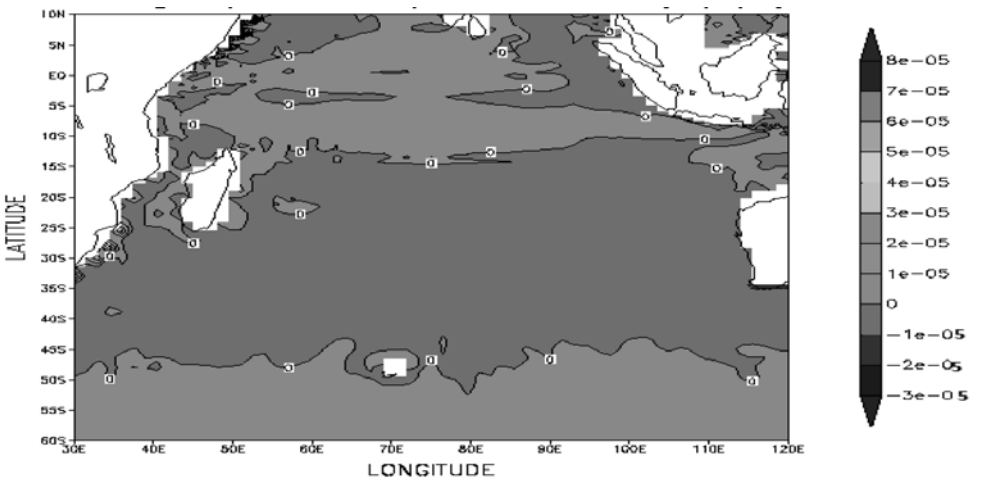

Figure 2. (b) Vertical velocity (m/s) at 97.5 m. The contour interval is $1X10^{-5}$ m/s in vertical velocity. Negative VV shows the downslope flows.

region. The high surface elevation field is associated with equatorial Indian Ocean/North Indian Ocean up to 25°S while the low elevation fields are seen near Antarctica Circumpolar Region (40°S-60°S). Moreover, the Sea level drop in Agulhas region is seen to be around 15-18 cm. In addition to such distribution, bump shaped frontal structure around Agulhas retroflexion area, 30°E (although area prior 30°E is not covered) can be understood and structure around the Antarctic Circumpolar Current (ACC) is well captured. Agulhas retroflexion is related to the Agulhas Current (27°S to 40°S, Gordon, 1985), a western boundary current of Southern Indian Ocean, since as it reaches the Southern Ocean, the current retroflects or turns back on itself and flows eastward with part of the flow recirculating in the counter clockwise flowing subtropical gyre and part of the flow feeding the Antarctic Circumpolar Current as Agulhas return Current (Quartly and Srokosz, 1993).

Figures 2a, 3a and 4a show the velocity field at 97.5 m, 875.5m and near the bottom, respectively averaged over the last six years of the simulation. The vertical velocity is diagnosed through the continuity equation; horizontal velocities are driven by the Coriolis force, horizontal pressure gradient and advection terms.

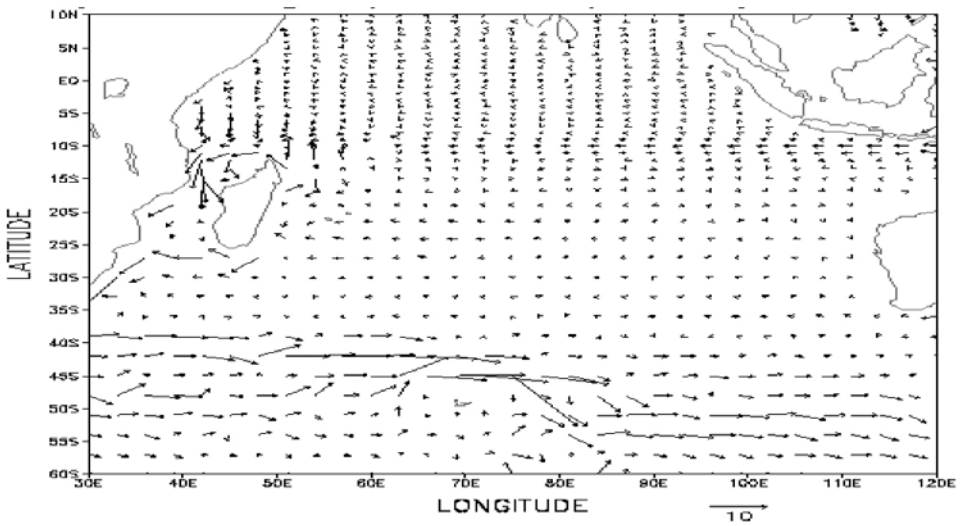

Figure 3. (a) Six year average horizontal circulation (cm/s) at 882m. In figure (a) arrow length of 0.5 cm represents current speed of 10 cm/s.

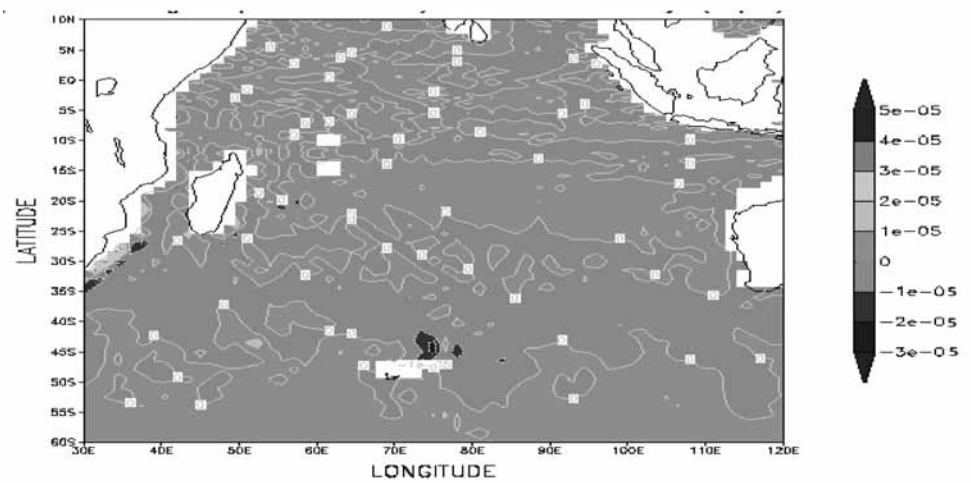

Figure 3. (b) Vertical velocity (m/s) at 882m. The contour interval is $1x10^{-5}$ m/s in vertical velocity. Negative VV shows the downslope flows.

At 97.5 m depth the dominant features are the westward and eastward flow of Southward Equatorial Current (SEC) and the Antarctic Circumpolar (ACC) flow respectively. Agulhas current is also revealed but various other currents viz; North Equatorial Current (NEC), Equatorial Counter Current (ECC) etc are not seen well and are too weak in the model (Figure 2a). The vertical velocity field shows the expected downward flow in the middle latitude from the wind driven Ekman pumping (Figure 2b). The horizontal flow field at 882m (Figure 3a) shows several small scale gyres in the Southern Ocean south of ACC. At this depth, SEC, NEC, ECC is not seen well while ACC is evident. We note entrainment of slope water west of the Madagascar into the subsurface water of ACC. Areas of strong downwelling are found along western boundaries, equatorial region etc. (Figure 3b).

The bottom flow field at 4882m (Figure 4a) generally follow the bottom topography contour (Olber and Volker 1996) and is the result of Ekman veering to the left (right) of the mean flow in the north (south) hemisphere, producing an upslope and downslope component. In the ACC, currents are very sparse and show few gyre structures (Figure 4a). The region of downslope near bottom flow in figure 4b indicates areas of possible deep water formation. For more clarity, we have plotted the overall feature of the model to find its fidelity. The very small vertical velocity ($3x10^{-21}$m/s) shows that it is difficult to model bottom boundary layer correctly by z-level model, which is also suggested by Winton et al., 1998 in his studies. Overall, it is also evident in the figures 2a, 3a, 4a that strength of the subsurface currents at different depths is decaying monotonically down in comparison to the circulation in the preceding depths (e.g. 60cm/s at 97.5 m

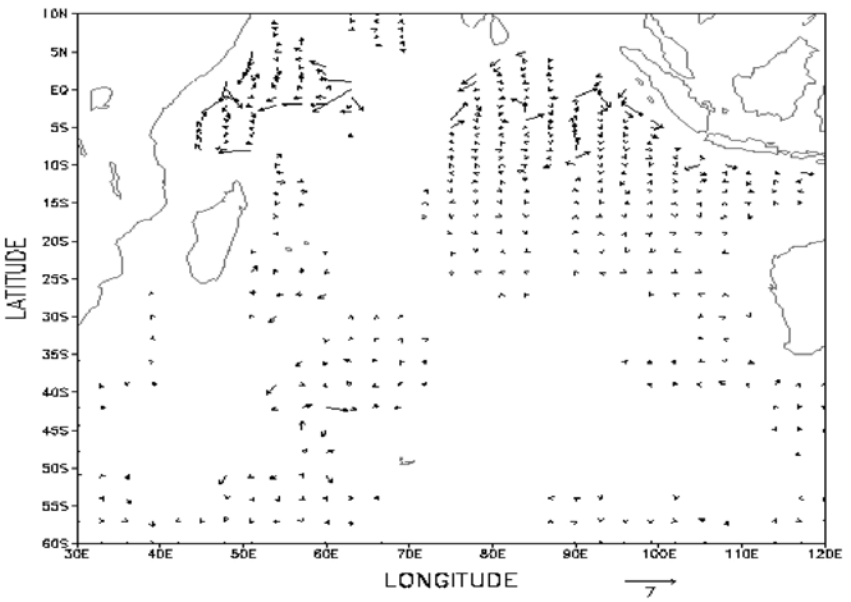

Figure 4. (a) Six year average horizontal circulation (cm/s) at 4482m. In figure (a) arrow length of 0.5 cm represents current speed of 7cm/s.

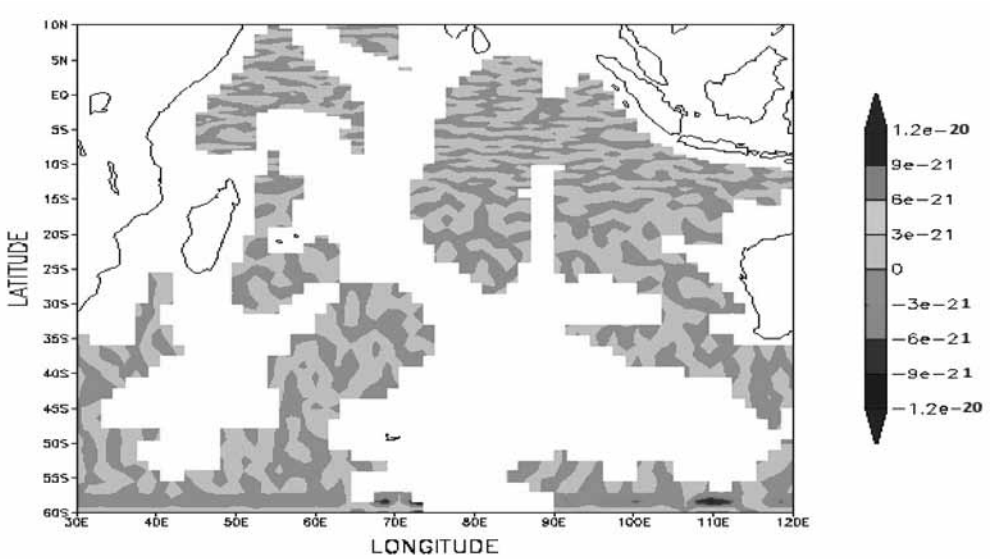

Figure 4 (b). Vertical velocity (m/s) at 4482 m. The contour interval is $3x10^{-21}$m/s in vertical velocity. Negative VV shows the downslope flows.

depth, 10cm/s at 882m depth and 7cm/s at 4482 m depth) which shows that subsurface currents travel at a much slower speed when compared to surface flows. This is in accordance with the study suggested by Pidwirny, 2006 and owing to stratified ocean, velocities tend to be faster near to the surface (Gille, 1994).

Upper Ocean Volume Transport

To examine the contribution of wind forcing, we have computed the upper ocean volume transport. The upper ocean volume transport quantifies the flow patterns with water column of subtropical waters implied by the volume transport sections and is distributed at 60°S at about 250m depth, with magnitude lying between +5Sv to -1Sv (1 Sv=10^6 m^3/s). In the figure 5, the Agulhas current is marching swiftly towards north and the flow is weak with zero (0) Sv net transports at 30°E. These exterior flows significantly differ from the flows continuing up to 120°E. However, the energetics between +5/-1 Sv flows through Mozambique ridge at 35°E and Madagascar ridge at 44°E and there seems to be variable contribution of transport

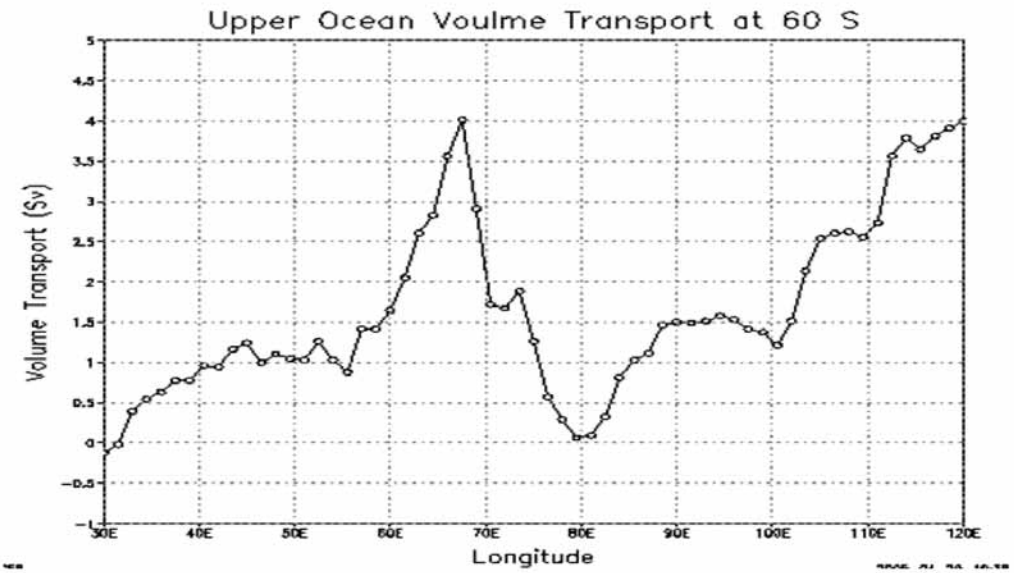

Figure 5. Upper ocean volume transport (Upper 250 meter depth) at 60°S in the region 30°E-120°E.

in feeding anticyclonic eddies on its left side as observed from incidence of different order (+5 Sv to -1 Sv). In the figure no 5, the fluctuations are confined to 250m depth, with a larger meridional scale width and in the upper ocean above the top of the thermocline, the zonal transports are eastward that may directly follow the surface currents. This result suggests that the vertically integrated, persistent eastward transport results largely from the layers in and below the thermocline (Weiqing et al., 2004).

Statistical Analysis between Model & Observed SST

Methodology and Formulation

For evaluation of the model results, monthly means are formed from January through December using the model years. These values are then compared to climatology at each grid point of the model domain. Several statistical measures are considered together to assess the comparisons between SST values predicted by the model and those predicted by the observed SST data (Levitus 1994). Here, we have taken the region of interest 60°S-20°N, 30°E-120°E to discuss SST analysis in detail.

Let Xi (i=1, 2,.....,n) be the set of n reference values (i.e. observed SST, Levitus, 1994) and let Yi (i=1, 2,.....,n) be the set of estimates (i.e. Model SST). Also let $\overline{X}$ and $\overline{Y}$ and σ_x and σ_y be the mean and standard deviations of the reference (estimate) values respectively. For model data comparisons, we evaluate time series of monthly mean SST values from January to December at each grid point over the domain, so n is 12.

We have used the following statistical relationship between observed SST (X) and Model SST(Y) [based on Stewart (1990) and Murphy (1988) formula] as follows and also described by Kara, Wallcraft and Hurlburt 2003]:

$$ME = \overline{Y} - \overline{X} \tag{1}$$

$$RMS = \left[\frac{1}{n}\sum_{i=1}^{n}\left(Y_i - X_i\right)^2\right]^{1/2} \tag{2}$$

$$R = \frac{1}{n}\sum_{i=1}^{n}\frac{\left(X_i - \overline{X}\right)\left(Y_i - \overline{Y}\right)}{\left(\sigma_x \sigma_y\right)} \tag{3}$$

$$SS = 1 - \frac{RMS}{SD^2} \tag{4}$$

where ME is the bias or annual mean difference (in ^{0}C), RMS is the root mean square difference (in ^{0}C), R is the correlation coefficient, SS is the skill score (in degree C), SD is the standard deviation (in ^{0}C) and SS is dimensionless. The skill score is understood to be a very informative tool of model performance in predicting SST since it takes bias into account and often used to assess the accuracy of forecasts produced by numerical, statistical, and/or conceptual models relative to the accuracy of forecasts based on simple forecasting methods such as climatology or persistence (Murphy, 1996).

We have examined the model SST with respect to climatology for Model Error (Figure 7) i.e. departure of model SST from the observation using equation 1, RMS difference using equation 2, Correlation Coefficients denoted by R using equation 3 (Figure 6) and Skill Score (SS) over the model domain. The RMS difference between

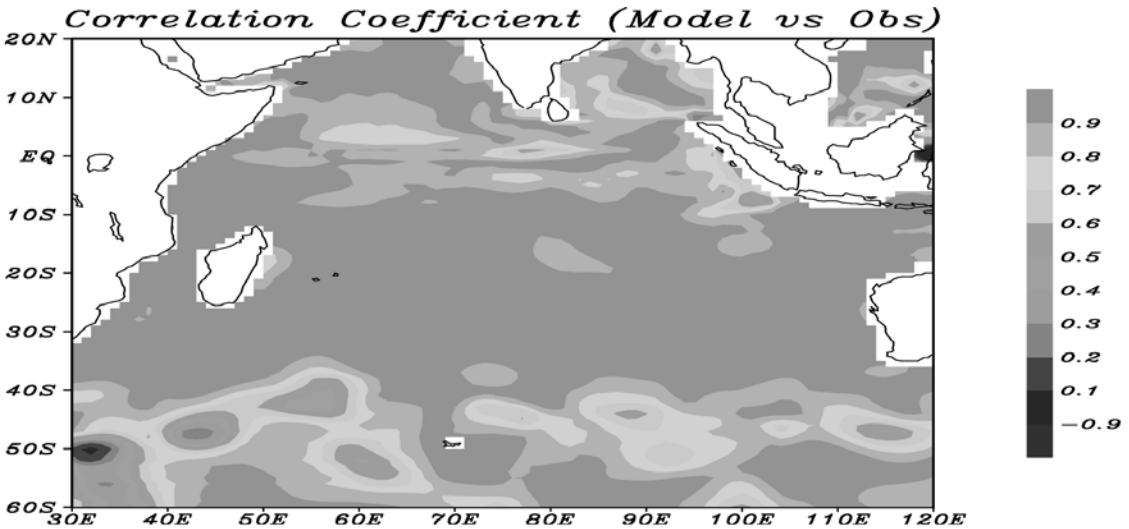

Figure 6. Correlation Coefficient (R) between model and observed SST.

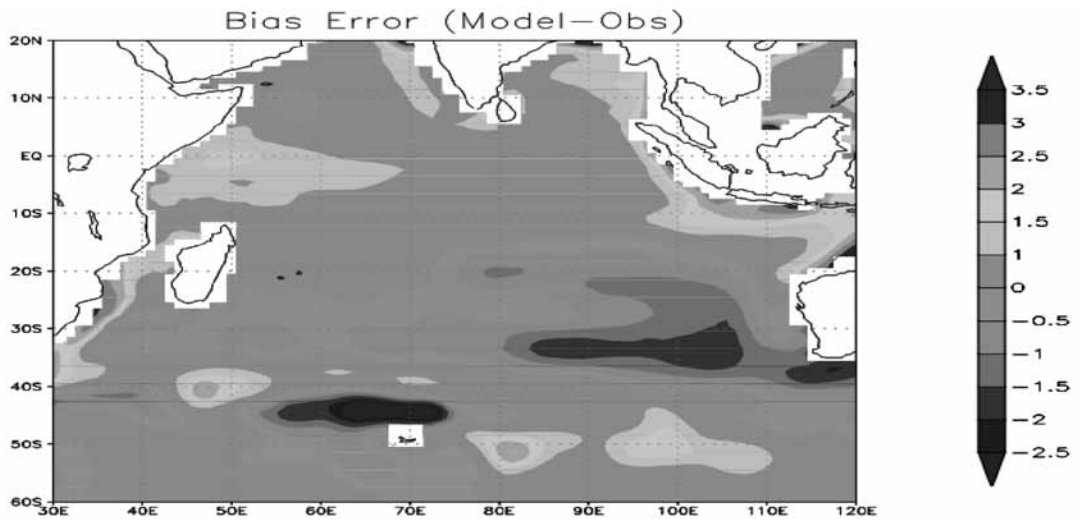

Figure 7. Annual mean error between model and observed SST. We note that mean error is between 0 to 1^0C in the model domain.

model and observed SST is 1.34^0C, Correlation Coefficients is 0.94, standard deviation between model and observed data is 1.15^0C respectively. The domain average skill score is found to be 0.59, yet not very high, but suggests the success of model up to some extent. As seen from the R values, which are close to 1 over most of the model domain, is thought to be SST is simulated well.

Although the correlation is very high between model and observed SST in the most part of the southern ocean and equatorial warm pool, the model SST seems to be simulated well as evident from R values (Figure 6), especially in the ACC region, the correlation seems moderate to high. In general, SST bias (model error) in figure 7 looks within 0 to 1^0 C, when compared to the observations in most part of the study region, which may be because of advection of colder surface water by upwelling processes. The SST errors in the open ocean are seen usually smaller than those along continental boundaries as well as upwelling regions. Cold SST biases are found in Southern Ocean around 20°S/40°S (Figure 7). Strong cooling by latent heat flux loss occurs in the central parts of the ocean (around 45°S/70°E) which may be due to strongness of the northeast trades and the weakness of south pacific convergence zone. In the present model study, the ocean temperature and salinity were restored to the observations, which could greatly improve the persistent bias. However, we would expect this bias to be improved in the high resolution model. In addition, it is also important to note that SST errors (Figure 7) along the continental boundaries may be due to steep structure of z-level models as suggested by Mellor et al., 2002; and Winton, Hallberg and Gnanadesikan, 1998).

SUMMARY AND CONCLUSIONS

The primary motivation of this study is to evaluate the coarse resolution ocean model around SIO/SO. As far as modelling results are concerned, they are providing a good source of information on the model outputs viz; circulation, its energetic property transports, etc. including quantitative & statistical estimation of model SST against the observed data set. Success of the model SST is revealed well by the high correlation coefficient (R=0.94) over the region of study, however, model is unable to predict/estimate VV for bottom boundary layer as the magnitude of VV is very small in the bottom. Its measurements are scarce because for, many years, velocity data in the ocean were collected primarily with mechanical current meters designed to measure the two horizontal component of velocity due to reasons of instrument cost and complexity (Thurnherr, 2011).

The model has always certain limitations and model provide its solution under a specified forcing under those limitations. However, forcing used in this Ocean General Circulation Model (OGCM) uses NCEP/NCAR climatological wind forcing which itself was regarded as less accurate forcing fields (Behra et al., 2000), due to which ocean modellers often relax ocean model simulation to the observed forcing. Hence, future step may be to use a coupled ocean atmosphere model to determine the implications on the finding presented here. Additionally, it is important to understand the uncertainty associated with the OGCM's simulation for statistical studies in respect of biases/error. In the modelling context, reproducing these results with OGCM's other than present set up with a coupled ocean–atmosphere model would be a valuable next step.

ACKNOWLEDGEMENTS

We gratefully acknowledge Dr. Bohua Huang and Dr. Ben Kirtman of Center of Ocean Land Atmosphere Studies (COLA), Maryland, USA for providing the MOM source code and forcing fields for the model runs. We are very much thankful to COLA for providing the model source code. As, the work was funded by National Centre for Antarctic and Ocean Research, Goa (now under Ministry of Earth Sciences, Government of India) we would like to thank NCAOR for providing the assistance and valuable suggestions from time to time. The constructive comments and suggestions made by anonymous reviewers helped us to improve the manuscript. The authors are also thankful to Dr.M.R.K.Prabhakar Rao and Chief Editor for apt editing of the manuscript.

Compliance with Ethical Standards

The authors declare that they have no conflict of interest and adhere to copyright norms.

REFERENCES

Adcroft, A., Hill C., and Marshall, J., 1997. Representation of topography by shaved cells in a height coordinate ocean model, Mon. Wea. Rev., v.125, pp: 2293–2315.

Best, S. E., Ivchenko V. O., Richards K. J., Smith R. D., and Malone, R. C., 1999. Eddies in Numerical Models of the Antarctic Circumpolar Current and their influence on the Mean flow, J. Phys. Oceano., v.29, pp: 328-350.

Behra, S. K., Salvekar, P. S., and Yamagata, T., 2000. Simulation of Interannual SST Variability in the Tropical Indian Ocean, J. Clim., v.13, pp: 3487–3499.

Gent, P. R., and McWilliams, J. C., 1990. Isopycnal mixing in ocean circulation models, J. Phys. Oceano., v.20, pp: 150–155.

Gerdes, R., 1993. A primitive equation ocean circulation model using a general ertical coordinate transformation. 1. Description and testing of the model; J. Geophys. Res., v.98, pp: 14,683-14,701.

Gille, S. T., 1994. Mean sea surface height of the Antarctic Circumpolar Current from Geosat data: Method and application, J. Geophys. Res., v.99, pp: 18255-18273.

Gnanadesikan, A., and Pacanowski, R., 1997. Improved representation of flow around topography in the GFDL Modular Ocean Model MOM2, Int. WOCE Newsl., v.27, pp: 23–25.

Gordon, A. L., 1985. Indian-Atlantic transfer of thermocline water at the Agulhas Retroflection, Science, v.227, pp: 1030-1033.

Huang, B., and Schneider, E. K., 1995. The response of an ocean general circulation model to surface wind stress produced by an atmospheric general circulation model. Mon. Wea. Rev., v.123, pp: 3059-3085.

Kalnay, E., and Co-authros., 1996. The NCEP/NCAR 40 year Reanalysis Project, Bull. Amer. Meteor. Soc., v.77, pp: 437-471.

Kara, A. Briol., Wallcraft A. J., and Hurlburt, H. E., 2003. Climatological SST and MLD Prediction from a Global Layered Ocean Model with an Embedded Mixed Layer, J. Atmos. and Ocean Techno., v.20, pp: 1616-1632.

Killworth, P. D., and Nanneh, M. M., 1994. Isopycnal Momentum Budget of the Antarctic Circumpolar Current in the FRAM, J. Phys. Oceanogr., v.24, pp: 1201-1223.

Large, W. G., McWilliams J. C., and Doney, S., 1994. Oceanic vertical mixing: A review and a model with nonlocal boundary layer parameterization, Rev. of Geophys., v.32, pp: 363-404.

Levitus, S., 1982. Climatological Atlas of the World Ocean 1982, NOAA (US Government Printing Office, Washington D C)., Report No. 13, pp: 173.

Levitus, S., and Boyer, T. P., 1994a. World Ocean Atlas 1994, Oxygen. NOAA Atlas NESDIS 2, U.S. Department of Commerce, NOAA, NESDIS., v.2.

Levitus, S., Burgett R., and Boyer, T. P., 1994b. World Ocean Atlas 1994, Salinity. NOAA Atlas NESDIS 3, U.S. Department of Commerce, NOAA, NESDIS., v.3.

Mellor, G. L., Hakkinen, S., Ezer, T., and Patchen, R., 2002. A generalization of a sigma coordinate ocean model and an intercomparison of model vertical grids, In: Ocean Forecasting: Conceptual Basis and Applications, N. Pinardi and J. D. Woods (Eds.), Springer, pp: 55-72.

Mishra, A. P., Rai S., and Pandey, A. C., 2010. Ocean Model derived global surface circulation and vertical velocity, J. of Geolog. Soc. India, v.76, pp: 468-478.

Munk, W., 1990. The Heard Island Experiment Naval Research Reviews; v.42, pp: 326-369.

Murphy, A. H., 1996. General decompositions of MSE-Based Skill Scores: Measures of some basic aspects of Forecast quality, Mon. Wea. Rev., v.124, pp: 2353-2369.

Murphy, A. H., 1988. Skill scores based on the mean square error and their relationships to the correlation coefficient, Mon. Wea. Rev., v.116, pp: 2417-2424.

Olber, D., and C. Völker, 1996. Steady states and variability in oceanic zonal flows. Decadal Climate Variability: Dynamics and Predictability, D. L. T. Anderson and J. Willebrand, Eds., Springer-Verlag, pp: 407–443.

Pacanowski, R. C., Dixon, K., and Rosati, A., 1993. The GFDL Modular Ocean Model user guide, version 1.0, Technical Report 2, Geophys. Fluid Dyn. Lab., National Oceanic and Atmospheric Administration, Princeton, New Jersey, pp: 16.

Pidwirny, M., 2006. Surface & subsurface Ocean Currents Fundamentals of Physical Geography, 2nd edition. (http://www.physicalgeography.net/fundamentals/8q.html).

Quartly, G. D., and Srokosz, M. A., 1993. Seasonal variations in the region of the Agulhas retroflection: Studies with Geosat and FRAM, J. Phys. Oceanogr., v.23, pp: 2107–2124.

Redi, M. H., 1982. Oceanic isopycnal mixing by coordinate rotation, J. Phys. Oceanogr., v.12, pp: 1154–1158.

Reynolds, W. R., Rayne, N. A., Smith T. M., Stokes, D. C. and Wang, W., 2002. An improved In Situ and Satellite SST Analysis for Climate, J. Climate., v.15, pp: 1609-1625.

Schneider, E. K., Huang B., Zhu Z., DeWitt D. G., Kinter III J. L., Kirtman, B., and Shukla, J., 1999. Ocean data assimilation, initialization, and predictions of ENSO with a coupled GCM, Mon. Wea. Rev., v.127, pp: 1187-1207.

Sheng, J., Wright D. G., Greatbatch, R. J., and Dietrich, D. E., 1998. CANDIE: A New Version of the DieCAST Ocean Circulation Model, J. Atmospheric and Ocean Technology., v.15, pp: 1414-1432.

Smagorinsky, J., 1963. General circulation experiments with the primitive equations: I. The basic experiment, Mon. Weather Rev., v.91, pp: 99–164.

Stewart, T. R., 1990. A decomposition of the correlation coefficient and its use in analyzing forecasting skill, Wea. Forecasting. v.5, pp: 661-666.

Thurnherr, A. M., 2011. Vertical Velocity from LADCP Data. Division of Ocean and Climate Physics; Journal of Atmosphere and Ocean Technology, 28:6, Lamont-Doherty Earth Observatory, Palisades, NY 10964.

Winton, M., Hallberg, R., and Gnanadesikan, A., 1998. Simulation of density driven frictional downslope flow in z-coordinate ocean model, J. Phys. Oceanogr, v.28, pp: 2163-2174.

Weiqing, Han., Webster P., Lukas, R., and Hacker, Hu. Aixue., 2004. Impact of Atmospheric Intraseasonal Variability in the Indian Ocean: Low-Frequency Rectification in Equatorial Surface Current and Transport, J. Phys. Oceano., v.34, pp: 1350-1372.

Wyrtki, K., 1981. An estimate of equatorial upwelling in the Pacific. *J. Phys. Oceanography.*, v.11, no.9, pp: 1205-1214.